— 1 —

Magnetic reconnection

Magnetic reconnection (MR) occurs in electrically conducting plasma where :

- magnetic topology of the magnetic field lines is rearranged
- magnetic ennergy is converted in particle energy, that is both thermal and flow energy

MR can disconnect formerly connected magnetic field lines like in the solar photosphere ([Giovanelli, 1947]) and MR can connect formerly disconnected magnetic field lines like in stellar wind-magnetosphere interaction ([Dungey, 1961]).

The first quantitative models of reconnection were based on the resistivity of the medium to break the frozen-in theorem of ideal MHD. The models of [Sweet, 1958] & [Parker, 1957] and [Petschek, 1964] were historically the most important. With the paper of [Harris, 1962], we had the first kinetic equilibrium of a current sheet associated to a magnetic field reversal, where magnetic reconnection can grow. Then, the paper of [Furth et al., 1963] laid the groundwork for the resistive tearing mode, and the letter of [Coppi et al., 1966] the one for the collisionless tearing mode.

1.1 The first reconnection models

A simple calculation can put forward what is needed (and mandatory) for magnetic reconnection to occur in a plasma.

A magnetic field line can be materialized by the center of gyration of a charged particle (when no E field is applied). The velocity of the B field is hence the one of the HT frame where $E_\perp$ is null. This velocity writes $\mathbf{V}_{\mathrm{HT}} = \mathbf{E} \times \mathbf{B}/B^2$ for a non-relativistic Lorentz transform. In ideal MHD,

$$\mathbf{E} = -\mathbf{U} \times \mathbf{B} \tag{1.1}$$

i.e. plasma and magnetic field are comoving : this is the Alfvén theorem of the frozen–in flux.

Notation 1. *Let* $\mathbf{E}^\star$ *be the non-ideal part of the electric field, ie* $\mathbf{E} = -\mathbf{U} \times \mathbf{B} + \mathbf{E}^\star$

What are the conditions on $\mathbf{E}^\star$ to allow reconnection ?

Let 2 (infinitely) close points A and C be on a same magnetic field line $\mathbf{B}$ and defining $\mathbf{L} = \overrightarrow{AC}$, that is $\mathbf{L}\times\mathbf{B} = 0$ (see Fig. 1.1). Under which condition do we have $\mathrm{d}_t(\mathbf{L}\times\mathbf{B}) = \mathrm{d}_t\mathbf{L}\times\mathbf{B}+\mathbf{L}\times\mathrm{d}_t\mathbf{B} = 0$?

The calculation should give you that in 2D reconnection can develop with a parallel irrotational electric field

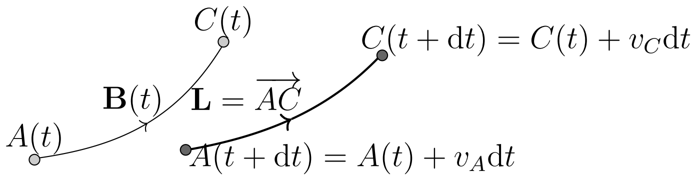

Figure 1.1: Advection of two close-by points on a magnetic field line.

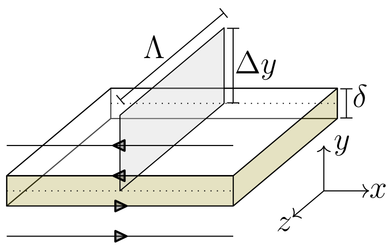

Figure 1.2: Geometrical limit of the magnetic flux above a current sheet.

$$\boldsymbol{\nabla} \times \mathbf{E}^{\star}_{\parallel} \neq 0 \tag{1.2}$$

This result is important because it puts forward that at the loci where magnetic field lines are de-connected/re-connected, such $E^{\star}$ should exist and its physical origin needs to be identified.

Before addressing these models, lets point-out how the efficiency of magnetic reconnection can be evaluated.

Reconnected flux and reconnection rate

Let $\mathrm{d}\Phi = \mathbf{B}.\mathrm{d}\mathbf{S}$ be the differential magnetic flux across a surface $\mathrm{d}\mathbf{S}$. Magnetic reconnection will only develop in current sheets where there is a large enough magnetic shear. The magnetic field reversal is given by

$$B_x(y) > 0 \quad \forall \quad y < 0 \tag{1.3}$$

$$B_x(y) < 0 \quad \forall \quad y > 0 \tag{1.4}$$

and is associated to a thin current sheet.

We focus on the magnetic flux through the surface $\Lambda\Delta y$ indicated in light gray in Fig. 1.2. The partial time derivative of the magnetic flux writes

$$\partial_t\Phi = \frac{B\Lambda\Delta y}{\Delta t} \tag{1.5}$$

The time-derivative of this flux is associated to the transport of B (along x) advected at the plasma velocity U (along y) by the E field (along z). The advection of B at the velocity U results

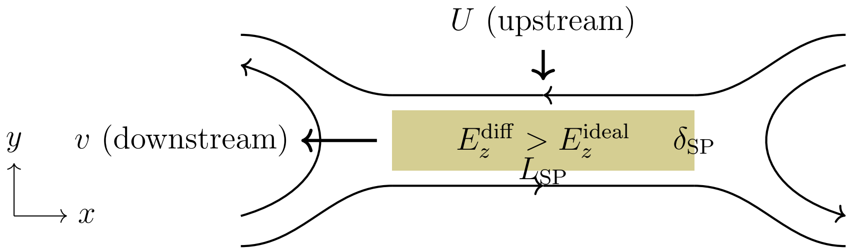

Figure 1.3: 2D geometry of the Sweet-Parker model.

from the frozen-in condition in the plasma, far above the CS where MHD is ideal. The Maxwell-Faraday equation gives

$$\partial_t \iint \mathbf{B}.\mathrm{d}\mathbf{S} = \iint (\boldsymbol{\nabla} \times \mathbf{E}).\mathrm{d}\mathbf{S} = \int \mathbf{E}.\mathrm{d}\mathbf{l} \tag{1.6}$$

i.e. $\partial_t \Phi = E\Lambda$. With the same upward flow below the $y = 0$ plane, we have the condition $E = 0$ at $y = 0$. Then, $E = B\Delta y/\Delta t = BU$ where U is also the fluid velocity in the frozen-in condition. This electric field E can be normalized using B_0 and A_0, *i.e.*

$$E' = \frac{E}{B_0 A_0} = \frac{U}{A_0} \tag{1.7}$$

Definition 1. *A_0 is the Alfvén velocity with the upstream asymptotic B_0 and ρ_0 values*

It clearly appears that this is a creation rate of flux upstream from the CS. For stationary reconnection, this flux is expelled by reconnection, so that creation rate $\equiv$ reconnection rate.

Definition 2. *E' is the reconnection rate and is not limited to the 2D case.*

Magnetic reconnection has to do with the decoupling between the magnetic field and the plasma. While such decoupling can be achieved by magnetic diffusivity, this phenomena is oftenly a very slow and ineffective process, because of the small magnetic diffusivity (the plasma resistivity, is very small in most space and astrophysical plasmas).

As a consequence, many efforts have been dedicated to reconnection model. The first resistive model, the one of Sweet & Parker involves the resistivity of the plasma, but is more than pure diffusion of the magnetic field.

The Sweet-Parker model

This is the first theoretical model of magnetic reconnection : Sweet suggested in a 1956 conference [Sweet, 1958] the role of resistive diffusion in a resistive current sheet and Parker wrote the associated equations [Parker, 1957] using conservation laws. The geometry of this model is depicted in Fig. 1.3.

As many theoretical models, the solution of this problem consist in finding the forme of the fluid flow in the upstream region where the ideal term in the Ohm's law is leading, the form of this same flow in the diffusion region where diffusive effects (that is collisions) are leading, and then find the way to continuously connect these flows together. Hence :

- In the upstream region, the frozen-in theorem is valid so the ideal Ohm's law gives $E_z = UB_0$
- In the diffusion region, plasma effects are dominated by collisions so $E_z = \sigma^{-1} J_z$

At MHD scales, $\omega/k \ll c$ meaning that the displacement current can be neglected. Hence,

$$(\boldsymbol{\nabla} \times \mathbf{B}).\hat{\mathbf{z}} = \mu_0 J_z \simeq \frac{B_0}{\delta_{\mathrm{SP}}} \tag{1.8}$$

meaning that in the diffusion region,

$$E_z = \frac{B_0}{\mu_0 \sigma \delta_{\mathrm{SP}}} \tag{1.9}$$

For a stationnary 2D process, $\partial_t B_x = \partial_t B_y = 0$, so that E_z is constant across the current sheet : the electric field in the diffusion region $E_z^{\mathrm{diffusion}} = J_z/\sigma$ has then to be equal to the electric field far upstream from the current sheet, that is in the ideal region where $E_z^{\mathrm{ideal}} = UB_0$. As a consequence,

$$U = \frac{1}{\mu_0 \sigma \delta_{\mathrm{SP}}} = \frac{\eta}{\delta_{\mathrm{SP}}} \tag{1.10}$$

Remark 1. *This form of U is equal to the diffusion velocity, as $\eta = l^2/\tau$, then*

$$v_{\mathrm{diff}} = \frac{l}{\tau} = \frac{\eta}{l} \tag{1.11}$$

with $l = \delta_{\mathrm{SP}}$

The upstream velocity U is very important as it is quantifying the reconnection efficiency (see Eq. 1.7). It is related to the geometry of the flow in the continuity equation

$$UL_{\mathrm{SP}} = v\delta_{\mathrm{SP}} \tag{1.12}$$

We then need an extra condition to get the value of the downstream flow v. It is going this way because both L_{SP} and δ_{SP} are geometric parameters of the flow and the SP model don't expect to provide their quantitative value. The downstream flow v can then be obtained from the pressure balance. In the upstream region, the inflow velocity U is quite small so that the pressure is essentially magnetic

$$\frac{B_0^2}{2\mu_0} \tag{1.13}$$

and in the downstream region where the magnetic field is vanishing, the pressure is essentially kinetic

$$\frac{1}{2}\rho v^2 \tag{1.14}$$

The pressure balance then writes

$$\rho v^2 = \frac{B_0^2}{\mu_0} \tag{1.15}$$

that is $v = A_0$: the outflow is Alfvénic (assuming a uniform density across the CS)

Remark 2. *In magnetic reconnection, any reference to an Alfvén velocity is always done using the upstream conditions.*

The electrical conductivity σ is measured in S.m^{-1}. But as a purely personnal choice, the magnetic diffusivity η related to σ with the relation

$$\eta = \frac{1}{\mu_0 \sigma} \tag{1.16}$$

is more pleasans to manipulate : because its unity is in m^2.s^{-1}, and because it quantifies the diffusion of the magnetic field across the plasma. Then,

$$\delta_{\mathrm{SP}} = \frac{\eta}{U} \tag{1.17}$$

so that one obtains

$$\frac{U^2}{A_0^2} = \frac{\eta}{L_{\mathrm{SP}} A_0} = \frac{1}{S} \tag{1.18}$$

Definition 3. *S is the Lundquist number : it is the ratio between the alfvén time and the diffusive time. Ii is also the magnetic Reynolds number if one considers the Alfvén velocity as the caracteristic velocity of the flow.*

The reconnection rate is then

$$E' = \frac{U}{A_0} = \frac{1}{\sqrt{S}} \tag{1.19}$$

so the simple geometric relation $\delta_{\mathrm{SP}} = L_{\mathrm{SP}} E'$. To set orders of magnitude, $S \sim 10^8$ in solar flares and $S \sim 10^{11}$ in the solar wind/Earth magnetosphere, which are quite large values, then giving a very small reconneciton rate. For these reasons, such reconnecting mechanicm is called "slow reconnection".

Remark 3. *The SP regime is called collisional as the Alfvén time associated to the length L_{SP} is larger than $\tau_{\mathrm{collision}}$*

As a result, any length, hence the CS thickness, is larger than d_i : $\delta_{\mathrm{SP}} > d_i$. Furthermore, when the plasma is expelled, it is frozen in the plasma, so it drives the B field out of the reconnection region. As a consequence, L_{SP} is growing meaning that the CS is getting elongated. This is not part of the SP model, but it has been verified experimentally and numerically.

During the increase of L_{SP} (decrease of S), the CS elongates until being unstable to secondary islands at $S_{\mathrm{crit}} \sim 10^4$. This regime will be discussed later in this chapter. For a uniform resistivity, simulation always produce a SP reconnection topology with a highly elongated diffusion region. In large collisional full-PIC [Daughton et al., 2009], for $\delta > d_i$, ρ_s, the SP-like CS grows hence getting elongated.

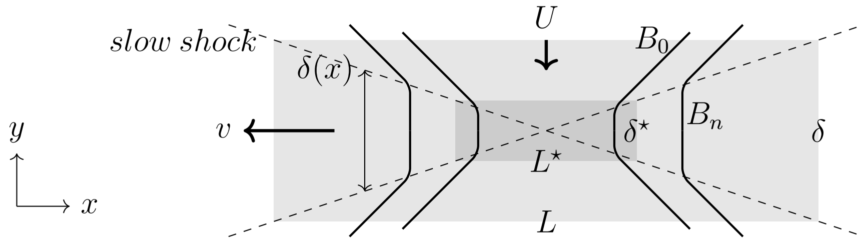

Figure 1.4: Schematic of the reconnection zone in the Petschek model

Remark 4. *The plasma inflow in SP is supposed laminar... if not, it could be the source of plasmoids [Lazarian and Vishniac, 1999].*

The Petscheck model

The Petscheck model starts with the topology of the Sweet-Parker model, but with an additional ingredient, which emphasizes the clear-sightedness of its author : in this model, there is still a dissipative zone in which the resistivity allows the topological reconfiguration of the magnetic field lines, but the plasma is not forced to pass through it! This eliminates the bottleneck of the Sweet-Parker model which is at the origin of its low reconnection rate. However, it will be necessary to find the process that will allow the acceleration of the plasma that no longer passes through the diffusion zone : it will be a slow shock.

Notation 2. *We introduce two characteristic scales in the plasma ejection direction : L is the characteristic dimension of the reconnection area, and $L^\star$ is the diffusion scale.*

In the Petschek model, the outflow region is much broader (between shock fronts of a slow shock) so the plasma is accelerated by the slow shock.

Notation 3. *In this model, the thickness $\delta(x)$ is an x-function, with a limit $\delta^\star$ in the diffusion region of length $L^\star \ll L$.*

Notation 4. *We define the dimensionless quantity $b_n = B_n/B_0 \ll 1$. We also remember that the reconnection rate is*

$$E' = \frac{U}{A_0} \tag{1.20}$$

Notation 5. *We also define two Alfvén velocity,*

$$A_n = \frac{B_n}{\sqrt{\mu_0 \rho}} \text{ and } A_T = \frac{B_T}{\sqrt{\mu_0 \rho}} \tag{1.21}$$

on each sides of the discontinuity (with respect to the normal)

Hypothesis 1. *We make the hypothesis of uniform ($\rho_0 \equiv \rho_1$) incompressible ($[V_n]_{\text{shock}} = 0$) plasma.*

The continuity equations writes

$$Ux = v(x)\delta(x) \tag{1.22}$$

for a uniform inflow velocity U (laminar hypothesis).

• Far from the diffusion region (upstream and downstream) but in the neighborhood of the shock : The jump equations for the tangential momentum in the HT frame writes

$$[(V_n^2 - \frac{B_n^2}{\mu_0\rho})\mathbf{B}_T]_{\text{shock}} = 0 \tag{1.23}$$

In the upstream region, $V_{n0} = U$, B_n is conserved and $B_{T0} \sim B_0$. In the downstream region, $\mathbf{B}_{T1} = 0$. As a result, the parenthesis in the upstream is null, that is

$$U^2 = \frac{B_n^2}{\mu_0\rho_0} \tag{1.24}$$

A first equation is then $E' = |b_n|$ which depends (as B_n) on x and y.

With the incompressible hypothesis, $[V_n]_{\text{shock}} = 0$ and $[B_n]_{\text{shock}} = 0$, so we have $[A_n]_{\text{shock}} = 0$. We then have the condition $V_n[\mathbf{V}_T]_{\text{shock}} = A_n[\mathbf{A}_T]_{\text{shock}}$ from the transverse momentum equation. V_n and A_n being conserved, we get $\mathbf{V}_{T0} - \mathbf{A}_{T0} = \mathbf{V}_{T1} - \mathbf{A}_{T1}$. With $V_{T0} \sim 0$, $A_{T0} \sim A_0$, $V_{T1} \sim v$ and $A_{T1} \sim 0$, we obtain

$$v = A_0 \tag{1.25}$$

as in the SP model. Note that v is then constant, *i.e.* does not depend on x. With the help of the continuity equation, $\delta(x) = E'|x|$ is linear.

• In the diffusion region :

The diffusion velocity writes

$$v_{\text{diff}} = \frac{\eta}{\delta^\star} = U \tag{1.26}$$

like in the SP model, to ensure the stationarity condition. A first condition is then

$$E' = \frac{\eta}{\delta^\star A_0} \tag{1.27}$$

so that

$$\delta^\star = \frac{\eta}{E' A_0} \tag{1.28}$$

which then defines the value of $\delta^\star$. A second condition is the relation between $L^\star$ and $\delta^\star$: for geometrical reasons,

$$\delta^\star = |b_n|L^\star = E'L^\star \tag{1.29}$$

In the diffusion region, b_n has to be an odd function of x, so we assume a linear form with

$$b_n(L^\star) = E' = \frac{\delta^\star}{L^\star} \tag{1.30}$$

hence

$$b_n(x) = \frac{(E')^3 A_0}{\eta} x \tag{1.31}$$

which is a first order approximation at the corner of the diffusion region, as well as

$$L^\star = \frac{\eta}{(E')^2 A_0} \tag{1.32}$$

The general solution has to continuously connect these 2 solutions in and out of the diffusion region. The form of the magnetic field $\mathbf{B}$ is solution of a Laplace equation with boundary conditions given by Eq. 1.31 at the shock.

The solution of the Laplace equation $\Delta \mathbf{B} = 0$ on D with $\mathbf{B}^\star(\mathbf{r}')$ given on $\mathbf{r}' \in \partial D$ is

$$\mathbf{B}(\mathbf{r}) = -\oint \mathrm{d}S' \mathbf{B}^\star(\mathbf{r}').\boldsymbol{\nabla} G_{\mathrm{HD}}(\mathbf{r}, \mathbf{r}') \tag{1.33}$$

where

$$G_{\mathrm{HD}}(\mathbf{r}, \mathbf{r}') = \frac{1}{4\pi |\mathbf{r} - \mathbf{r}'|} \tag{1.34}$$

is the Green function for homogeneous Dirichlet BC. The shock equation (in the first quadrant) being $y = E'x$, the integration gives

$$B_x(x,y) = -\frac{4E'B_0}{\pi} \ln \frac{L}{\sqrt{x^2+y^2}} \text{ and } B_y(x,y) = \frac{4E'B_0}{\pi} \arctan \frac{y}{x} \tag{1.35}$$

We then have

$$B_x(L^\star, \delta^\star) = -\frac{4B_0E'}{\pi} \ln \frac{L}{L^\star} \tag{1.36}$$

Eq. 1.37 relates the reconnection rate E', the geometry of the system (L and $L^\star$) and the magnitude of B_x at $(L^\star, \delta^\star)$ which is unknown.
The reconnection rate is then

$$E' = \frac{\pi B_x(L^\star, \delta^\star)}{4B_0} \frac{1}{\ln L/L^\star} \tag{1.37}$$

With $L^\star$ given by Eq. 1.32, and the arbitrary value $B_x(0, \delta^\star) = -\frac{1}{2}B_0$, one obtains

$$E' = \frac{\pi}{16} \frac{1}{\ln(E'S)} \tag{1.38}$$

Being in the Log, the E' in the rhs weakly contributes, so we have

$$E' \sim \frac{1}{\ln S} \tag{1.39}$$

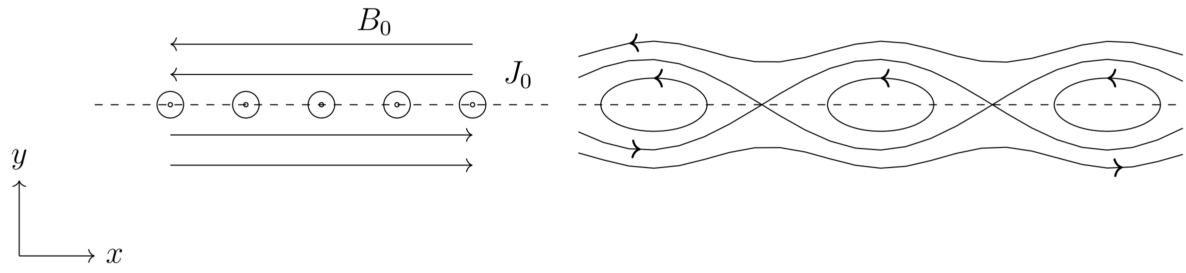

Figure 1.5: Schematic of a Harris sheet (left) and its evolution with the tearing mode (right)

It is the magnetic tension, important at the angular point, which ensures the acceleration of the plasma at the Alfvén speed. Through a slow shock, the normal velocity and tangential components of the magnetic field decrease, and the pressure and density increase. In the downstream flow zone, the magnetic field decreases by conservation of the flux. The kinetic pressure must therefore increase to satisfy the pressure balance, thus the heating of the plasma.

To increase the reconnection rate, it is necessary to increase the inflow speed U. However, this speed is not defined in a self-consistent way, and its relation with the magnetic field does not necessarily make it possible to reach a fast reconnection regime.

Petschek reconnection has been observed in-situ in the far geomagnetic tail ([Machida et al., 1994]) and is observed in simulation only for a highly localized resistivity (see eg. [Krauss-Varban and Omidi, 1995], [Ugai, 1999]).

1.2 The Harris kinetic equilibrium

In order to study magnetic reconnection, one must first describe the current sheet associated with the magnetic field reversal. The paper of [Harris, 1962], describes such a layer in the one-dimensional case. The left panel of Fig. 1.5 displays the shape of the magnetic field and the associated current.

A kinetic equilibrium is determined by the distribution function of each specie s as well as that of the associated electric and magnetic fields. This set must obviously satisfy the Vlasov equation (for each species s), as well as the stationary Maxwell equations. The resulting system is thus of the form

$$\mathbf{v}.\frac{\partial f_s}{\partial \mathbf{r}} + \frac{q_s}{m_s}(\mathbf{E} + \mathbf{v} \times \mathbf{B}).\frac{\partial f_s}{\partial \mathbf{v}} = 0 \quad (1.40)$$

$$\boldsymbol{\nabla}.\,\mathbf{E} = \frac{1}{\varepsilon_0}\sum_s \int_{\mathbb{R}^3} q_s f_s \, d\mathbf{v} \quad (1.41)$$

$$\boldsymbol{\nabla} \times \mathbf{B} = \mu_0 \sum_s \int_{\mathbb{R}^3} q_s f_s \mathbf{v} \, d\mathbf{v} \quad (1.42)$$

For a 1-dimensional equilibrium, the operators ∂_x and ∂_z are identically null. So the generalized canonical momentum P_x and P_z are constants of the motion. Moreover, the system is isolated (constant energy) and so the Hamiltonian H is also a constant of motion. The magnetic field is of the form $\mathbf{B} = B(y)\widehat{\mathbf{x}}$ and thus derives from a vector potential of the form

$$\mathbf{A} = A(y)\widehat{\mathbf{z}} \tag{1.43}$$

For each s particle specie, the invariants can be written (omitting the s index)

$$\begin{aligned} H &= {}^1\!/\!_2 m(v_x^2 + v_y^2 + v_z^2) + q\phi & (1.44)\\ P_x &= mv_x & (1.45)\\ P_z &= mv_z + qA(y) & (1.46)\end{aligned}$$

so we can deduce three new constants of motion for each s specie

$$\begin{aligned} \alpha_3 &= \frac{P_x}{m} = v_x & (1.47)\\ \alpha_2 &= \frac{P_z}{m} = v_z + q\frac{A_z}{m} & (1.48)\\ \alpha_1^2 &= 2\frac{H}{m} - \alpha_3^2 - \alpha_2^2 = v_y^2 - 2qv_y\frac{A_z}{m} - \frac{q^2A_z^2}{m^2} + 2q\frac{\phi}{m} & (1.49)\end{aligned}$$

For a system with three degrees of freedom (the three speed coordinates) a distribution function which only depends on the three constants α_1, α_2 and α_3 is by construction solution of the Vlasov equation. For a Maxwellian distribution with a density n_s, a bulk speed V_s (in the z direction) and a temperature T_s,

$$f_s(\alpha_1, \alpha_2, \alpha_3) = n_s\left(\frac{m_s}{2\pi k_B T_s}\right)^{3/2} \exp - \left[\frac{m_s}{2k_B T_s}(\alpha_1^2 + (\alpha_2 - V_s)^2 + \alpha_3^2)\right] \tag{1.50}$$

with

$$\alpha_1^2 + (\alpha_2 - V_s)^2 + \alpha_3^2 = v_x^2 + v_y^2 + (v_z - V_s)^2 + \frac{2q_s\phi}{m_s} - \frac{2q_sAV_s}{m_s} \tag{1.51}$$

The form of these distribution functions for each specie s is then integrated on $\mathbb{R}^3$ in the two Maxwell equations. These equations depend on the scalar and vector potentials. For the scalar potential,

$$\boldsymbol{\nabla} \times \mathbf{B} = \boldsymbol{\nabla} \times (\boldsymbol{\nabla} \times \mathbf{A}) = \frac{d^2A}{dy^2} \tag{1.52}$$

and for the scalar potential,

$$\boldsymbol{\nabla}. \mathbf{E} = \boldsymbol{\nabla}. (-\boldsymbol{\nabla}\phi) = -\frac{d^2\phi}{dy^2} \tag{1.53}$$

For a hydrogen plasma consisting of protons p and electrons e, of same density n and whose modulus of charge is e, after the integration of Eq. (1.41), the equation on ϕ is rewritten

$$\frac{d^2\phi}{dy^2} = \frac{en}{\varepsilon_0}\left\{\exp\left[-\frac{e\phi}{k_BT_p} + \frac{eAV_p}{k_BT_p}\right] - \exp\left[\frac{e\phi}{k_BT_e} - \frac{eAV_e}{k_BT_e}\right]\right\} \tag{1.54}$$

and Eq. (1.42) on A is rewritten

$$\frac{d^2A}{dy^2} = \mu_0 en\left\{V_p\exp\left[-\frac{e\phi}{k_BT_p} + \frac{eAV_p}{k_BT_p}\right] - V_e\exp\left[\frac{e\phi}{k_BT_e} - \frac{eAV_e}{k_BT_e}\right]\right\} \tag{1.55}$$

In the de Hoffman-Teller frame, the electric field is null : the temperatures and drift velocities of each specie s then satisfy

$$-\frac{V_e}{T_e} = \frac{V_p}{T_p} \tag{1.56}$$

Exercize 1. *Using a first order linearization of the momentum equation of specie s, show Eq. (1.56)*

With the new hypothesis $T_e = T_p$, the system writes for ϕ

$$\frac{d^2\phi}{dy^2} = \frac{en}{\varepsilon_0}\exp\left[\frac{eAV}{k_BT}\right]\left\{\exp\left[-\frac{e\phi}{k_BT}\right] - \exp\left[\frac{e\phi}{k_BT}\right]\right\} \tag{1.57}$$

and for A

$$\frac{d^2A}{dy^2} = \mu_0 enV\exp\left[\frac{eAV}{k_BT}\right]\left\{\exp\left[-\frac{e\phi}{k_BT}\right] + \exp\left[\frac{e\phi}{k_BT}\right]\right\} \tag{1.58}$$

$\phi = 0$ is solution for the first equation, so the second equation can be written

$$\frac{d^2A}{dy^2} = 2\mu_0 enV\exp\left[\frac{eAV}{k_BT}\right] \tag{1.59}$$

A solution for this equation satisfying $A = 0$ and $B = 0$ at $y = 0$ is of the form

$$A(y) = \Gamma\ln[\cosh(\eta y)] \tag{1.60}$$

By deriving twice and identifying the terms, we get

$$\Gamma = -\frac{2k_BT}{eV}\ , \quad \eta = \left(\frac{\mu_0 ne^2V^2}{4k_BT}\right)^{1/2} \tag{1.61}$$

that is, introducing the Debye length λ_D,

$$\eta = \frac{V}{2c\lambda_D} \tag{1.62}$$

The magnetic field is of the form

$$\mathbf{B} = (\mu_0 nk_BT)^{1/2}\tanh\left(\frac{Vy}{2c\lambda_D}\right)\widehat{\mathbf{x}} \tag{1.63}$$

By isolating the density term n in Eq. (1.59), one obtains

$$n(y) = n \cosh^{-2}\left(\frac{Vy}{2c\lambda_D}\right) \tag{1.64}$$

For the forthcoming calculations, we write L the half-width of the Harris sheet

$$L = \frac{2c\lambda_D}{V} \tag{1.65}$$

In this result, we can discuss several hypotheses, including choosing $\phi = 0$. This implies that in the current layer, the equilibrium is associated with no electric field. This point can be discussed, and the satellite measurements do not show it clearly. But it is a mathematically sympathetic hypothesis, often made by the few models of kinetic equilibrium of the current layer.

1.3 The collisional tearing mode

The collisional tearing mode is an example of resistive MHD instabilities. The idea is to write the minimum set of equations in order to describe the plasma configuration, and to find a solution as purely growig mode (in time) for a given wavenumber. The system of coordinate is the same as for the Harris equilibrium ; X is the main direction of the anti-parallel (unperturbed) magnetic field, Y is the normal direction where the gradient are explicit, and Z is the direction of the current.

We start withthe linear phase of the collisional tearing mode firstly discussed by [Furth et al., 1963]. In order to decrease the number of unknowns, and thus the number of equations, we describe the magnetic field using the Euler potential. The magnetic field is thus written using the two scalar potential $\alpha(\mathbf{r})$ and $\beta(\mathbf{r})$:

$$\mathbf{B}(\mathbf{r}) = \boldsymbol{\nabla}\alpha \times \boldsymbol{\nabla}\beta \tag{1.66}$$

Exercize 2. *Can you justify this choice ? Can we describe whatever magnetic field with such potential description ? Can you say why the magnetic field lines are then given by the intersection of the two surfaces $\alpha = Cst.$ and $\beta = Cst.$?*

The unperturbed magnetic field has a component in the X direction and the first order perturbations also have a component in the Y direction. Hence, the magnetic field can be written

$$\mathbf{B}(\mathbf{r}) = \boldsymbol{\nabla}\psi \times \hat{\mathbf{z}} + B_G\hat{\mathbf{z}} \tag{1.67}$$

In the above equation, B_G is a guide field, which plays no role in this instability. Noting B_0 the assymptotic magnetic field and $f(y)$ the analytical profile of the unberturbed magnetic field, we have $B_0 f(y) = \partial_y\psi_0$, and a first order ψ_1 quantity will also develop. The total current is then given by

$$\mathbf{J} = \frac{1}{\mu_0}\nabla^2\psi\hat{\mathbf{z}} \tag{1.68}$$

As we are looking for a purely growing mode, ψ_0 depends on y, and ψ_1 evolves as $e^{\imath kx}$. The laplacian operator then writes $\nabla^2 = \partial^2_{y^2} - k^2$.

In the same spirit, we chose to describe the velocity using a potential. As we search for a velocity in the XY plan (i.e. without a Z component), then

$$\mathbf{v} = \boldsymbol{\nabla}\phi \times \hat{\mathbf{z}} \tag{1.69}$$

Exercize 3. *Can you explain this choice ? Do we have enough degrees of freedom with this form ? Is there any associated constraint ?*

We then have a parametric form of the magnetic field, while the electric field is given by the resistive Ohm's law. We do not need any continuity equation for an incompressible plasma, and we will see later on that we do not need any closing equation for the pressure. We then have all the needed parameters. The next step is to write the Maxwell-Ampère equation :

$$\frac{\partial \mathbf{B}}{\partial t} = -\boldsymbol{\nabla} \times \left[-\mathbf{v} \times \mathbf{B} + \frac{\mathbf{J}}{\sigma} \right] \tag{1.70}$$

Using the Euler potentials, this equation can be written

$$\frac{\partial \psi}{\partial t} - \mathbf{v}.\boldsymbol{\nabla}\psi = \frac{1}{\mu_0 \sigma} \nabla^2 \psi \tag{1.71}$$

Exercize 4. *Demonstrate the form of Eq. (1.71).*

As the plasma velocity $\mathbf{v}$ appears in this equation, we need to write an equation giving its time evolution ; it is of course the momentum equation. Its curl gives

$$nm \left(\frac{\partial \nabla^2 \phi}{\partial t} + \mathbf{v}.\boldsymbol{\nabla}\nabla^2\phi \right) = \frac{\hat{\mathbf{z}}}{\mu_0} \left[\boldsymbol{\nabla}\psi \times \boldsymbol{\nabla}(\nabla^2 \psi) \right] \tag{1.72}$$

Exercize 5. *Is it now clear why we do not need any closure equation for the pressure ? is there any underlying assumption(s) ?*

The system of Eq. (1.71) and Eq. (1.72) drives the time evolution of the two scalars ϕ and ψ. As is, this system is not that simple to solve as it is differential in both space and time. But as already mentioned, we look at a solution with a wavenumber k in the X direction, we keep the explicit derivative in the Y direction (as we need to consider the form of $f(y)$), and we solve this system for a purely growing mode in $e^{\gamma t}$. After linearizing this sytem at first order, one obtains

$$\begin{aligned} \gamma\psi_1 + \imath k B_0 \phi_1 f(y) &= \frac{1}{\mu_0 \sigma} \left(\frac{\partial^2}{\partial y^2} - k^2 \right) \psi_1 && (1.73) \\ \gamma nm \left(\frac{\partial^2}{\partial y^2} - k^2 \right) \phi_1 &= \frac{\imath k B_0}{\mu_0} \left[\psi_1 \frac{\partial^2 f(y)}{\partial y^2} - f(y) \left(\frac{\partial^2}{\partial y^2} - k^2 \right) \psi_1 \right] && (1.74) \end{aligned}$$

We then need to distinguish two regions : far from the current sheet where the system is somewhat in ideal MHD conditions (i.e. $\sigma \to \infty$) and inside the current sheet, where the plasma is dominated by the diffusive processes.

In the MHD region : From Eq. (1.73), we have

$$\phi_1 = \imath \frac{\gamma}{kB_0} \frac{\psi_1}{f(y)} \tag{1.75}$$

combining with Eq. (1.74) we get

$$\left[\frac{d^2}{dy^2} - k^2 - \frac{1}{f(y)} \frac{d^2 f(y)}{dy^2}\right] \psi_1 = -\frac{(\gamma\tau_A)^2}{f(y)} \psi_1 \sim 0 \tag{1.76}$$

where we have introduced $\tau_A = (kv_A)^{-1}$, the characteristic Alfven time. As $f(y)$, ψ_1 and ϕ_1 are only depending on the Y coordinate, we change the partial derivative with respect to y in total derivative. Eq. (1.76) is close to zero, as we make the hypothesis that $\gamma\tau_A \ll 1$ (which will be verified at the end of the calculation).

It then appears that we have a singular point at $y = 0$ because $f(0) = 0$. As a consequence, ψ_1 is discontinuous at the origin $y = 0$. We then introduce a parameter to characterize this discontinuity, defined by

$$\Delta' = \frac{d_y\psi_1(0^+) - d_y\psi_1(0^-)}{\psi_1(0)} \tag{1.77}$$

Exercize 6. *With this definition, one can verify that $d_y B_y = \Delta' B_y$ at $y = 0$.*

In the diffusive region : ψ_1 and ϕ_1 are such that their second derivative with respect to y is very large compared to their respective product with k^2 (because of the discontinuities of their derivatives). Hence, the system of Eq. (1.73) and (1.74) can be rewritten

$$\gamma\psi_1 + \imath kB_0\phi_1 \frac{y}{L} \sim \frac{1}{\mu_0\sigma} \frac{d^2\psi_1}{dy^2} \tag{1.78}$$

$$\gamma nm \frac{d^2\phi_1}{dy^2} \sim -\imath \frac{kB_0}{\mu_0} \frac{y}{L} \frac{d^2\psi_1}{dy^2} \tag{1.79}$$

because we approximate $f(y) \sim y/L$ (valid in the very middle of the current sheet). We then need to make the connection between the two solutions, inside the diffusive region and in the MHD region.

At the edge of the layer : we note $y = W$ the edge of the diffusive layer. The second derivative of both ψ_1 and ϕ_1 can be written

$$\frac{d^2\psi_1}{dy^2} = \frac{\Delta'}{W} \psi_1 \tag{1.80}$$

$$\frac{d^2\phi_1}{dy^2} = \frac{1}{W^2} \psi_1 \tag{1.81}$$

At the edge $y = W$ of the layer, the three terms in the Maxwell-Ampère equation are then comparable, so

$$\gamma\psi_1 \sim \imath k B_0 \phi_1 \frac{W}{L} \sim \frac{1}{\mu_0\sigma}\frac{\Delta'}{W}\psi_1 \tag{1.82}$$

The momentum equation given by Eq. (1.79) can also be approximated by

$$nm\frac{\gamma}{W^2}\phi_1 \sim -\imath\frac{kB_0}{\mu_0}\frac{W}{L}\frac{\Delta'}{W}\psi_1 \tag{1.83}$$

With Eq. (1.82) and (1.83), we have $\left(\frac{W}{L}\right)^5 = \frac{\Delta' L}{S^2}$ where

$$S = \frac{\tau_R}{\tau_A} \tag{1.84}$$

is the Lundquist number, $\tau_A = L/v_A$ is the Alfven time and $\tau_R = L^2/\eta$ the resistive time. Then, the growth rate of the resistive tearing mode is

$$\gamma = \frac{(\Delta' L)^{4/5}}{\tau_R} S^{2/5} \tag{1.85}$$

It is important to note that in most of the space and astrophysical plasmas, S is very large, meaning that $\gamma^{-1} \ll \tau_R$. Even if the origin of the tearing mode is resistivity, it means that the associated reconnection process is much faster than the simple magnetic diffusivity. It is also important to note that the growth rate of the collisional tearing mode increase with L, i.e. the length of the current sheet.

In his seminal paper, [Loureiro et al., 2005] described in a quantitative way how this linear phase evolves with time. He studied the case of a large Δ'/low η current sheet, destabilized for $\Delta' > 0$. In such a strongly driven regime, the linear tearing mode develops as described by [Furth et al., 1963]. Then, its following non-linear phase is well described by [Rutherford, 1973] as a square law with time. During this phase, the two islands bordering the X-line have a width W that is growing until a critical value W_{critical}. At this stage, the X-line collapses, meaning that a current sheet is developing and elongating between the two islands. The fastest growth of W is observed during this last phase. The length L of this current sheet then increases with time, and during this phase, the reconnection process is the one described by [Sweet, 1958] and [Parker, 1957] with a growth rate $\gamma_{\text{SP}} \sim \eta^{\frac{1}{2}}$. The thickness of the current sheet $\delta \sim \eta^{\frac{1}{2}}$ leads to an aspcet ratio L/δ that grows with time, until a critical value around 50, observed numerically. In term of the Lundquist number, elongated SP layers are unstable to secondary magnetic islands (MATTHAEUS1985) for $S > S_{\text{critical}} \sim 10^4$,

Then, for such an elongated current sheet, the collisional tearing turns to be unstable, so that a new island (surrounded by two X-lines) is created in the elongated Sweet-Parker current sheet. This secondary island is attracted by the primary one, so will merge with the closest/larger of their neighbour. The process continues until no more magnetic flux is available, or when "monster plasmoids" will get this region too far from being a current sheet ready for reconnection. This happen for a critical value of W, at which the instability saturates, ending this chained process.

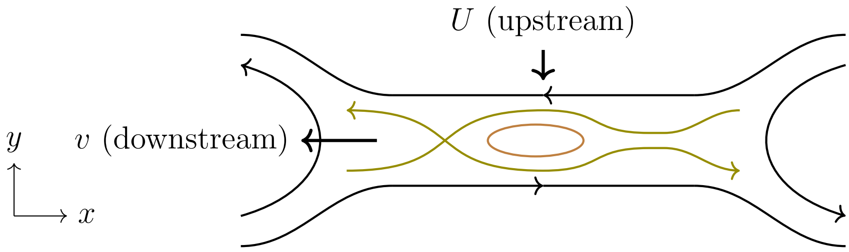

Figure 1.6: Time evolution of the topology of a SP current-sheet unstable to plasmoids.

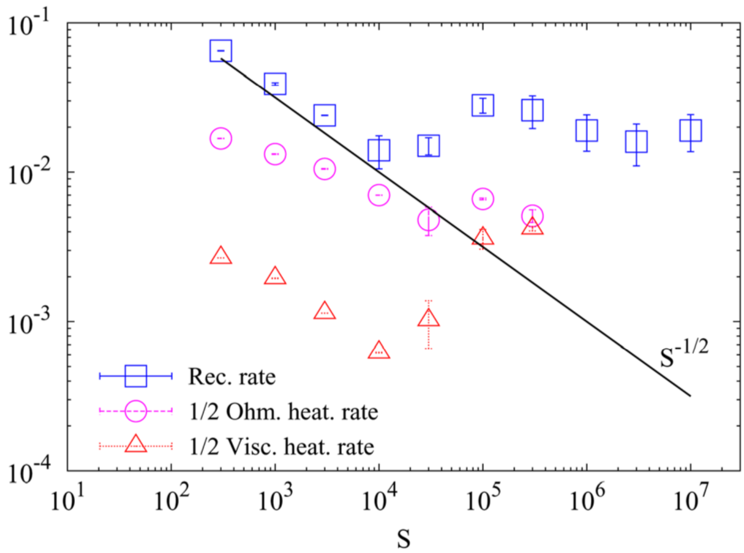

Figure 1.7: Time evolution of the reconnection rate (blue line) depending on the Lundqvits number S (see [Loureiro et al., 2012]).

[Loureiro et al., 2012] showed that for $S > 10^4$, the reconnection rate no longer decreases with a law in $S^{-1/2}$ as in the model of Sweet- Parker, but saturates at a value of about 10^{-2}, associated to $S_{\text{critical}} \sim 10^4$. This is illustrated in Fig. 1.7. Note that the definition of the reconnection rate must be reviewed in a system for which there is more than one reconnection site. Although not discussed in this document, the resistive tearing mode can therefore play a role in the formation of " plasma chain " in a thin and long current layer, even for a medium for which $S \to \infty$. The numerical results of [Loureiro et al., 2012] also show the possibility during the coalescence of these structures to create " monster plasmoids ".

1.4 The collisionless tearing mode

In a Harris sheet, the magnetic field depends only on the y coordinate. The stationary Maxwell-Ampère equation provides the current density required to maintain this magnetic topology,

$$\mu_0 \mathbf{J} = \boldsymbol{\nabla} \times \mathbf{B} \tag{1.86}$$

This magnetic field is associated with a current sheet in the direction $+\widehat{\mathbf{z}}$ located at $y = 0$ and of infinite extension in x and z directions as shown in the left panel of Fig. 1.5. This layer can be seen as an assembly of wires of parallel currents. There is hence an attractive force between each of these wires, whose modulus is inversely proportional to the square of their distance. An initial disturbance consisting in bringing together two close-by wires is therefore amplified, which reflects an unstable situation. However, it must be ensured that the quantity of energy available is sufficient. In addition, the current density accumulation involves a change in the topology of the field lines as shown in the right panel of Fig. 1.5, which is a priori not allowed by the frozen-in theorem.

We can give a qualitative answer to these two problems before demonstrating it analytically. To analyze the stability of the phenomenon, it is necessary to know if the energy released is higher than the one necessary to topologicaly modify the magnetic field lines. The energy released by the coalescence of current filaments depends on the length of the current sheet (in the X direction), whereas the modification of the shape of the magnetic field occurs on the thickness of the layer (in the Y direction). Since the length of the sheet is always greater than its thickness, there will always be an instability threshold for a sufficiently thin and long layer.

One then has to identify the physical argument(s) that no longer freeze the magnetic field in the plasma. Since the work of Landau, the effect that bears his name (and by which the particles whose distribution function f is such that $\partial_{\mathbf{v}} f > 0$ excite a wave with a positive growth rate) is a good candidate to produce diffusion. The situation in which a wave excites particles whose velocity is equal to or greater than the phase velocity of the wave also exists, and is often called the Čerenkov effect. It is by this effect that the waves produced by the tearing mode will accelerate the particles, and produce the diffusion sufficient to modify the magnetic field line connections.

For the development of the Čerenkov effect, the particles must be unmagnetized. In the opposite case, the cyclotronic motion associated with a magnetic field does not allow the resonance of the particles (or more exactly not the one associated with the Čerenkov effect). This is so because at y (the reference $y = 0$ is taken at the center of the layer) the local Larmor radius must be larger than y. By approximating the shape of the magnetic field at the center of the layer by a linear law, this inequality is written

$$|y| < l_s = \sqrt{\rho_s L} \tag{1.87}$$

where $\rho_s = v_{Ts}/\Omega_s$ is the Larmor radius of the thermal particles of species s, $v_{Ts} = \sqrt{k_B T_s / m_s}$ is the thermal velocity of the particles of species s and $\Omega_s = q_s B_0 / m_s$ is the cyclotron frequency of the species s in the asymptotic field B_0.

The problem is therefore simple : considering a perturbation of the magnetic field whose vector potential is of the form [1]

[1] This choice results from the shape of the magnetic field of order 0 and 1 that we are looking for

$$\mathbf{A}_1(x, y, t) = A_1(y)e^{-\imath(\omega t - kx)}\widehat{\mathbf{z}} \tag{1.88}$$

it has to satisfy the Maxwell-Faraday equation

$$\boldsymbol{\nabla} \times (\boldsymbol{\nabla} \times \mathbf{A}_1) = \mu_0 \mathbf{J}_1 \tag{1.89}$$

in which the right-hand side must include all the currents of order 1 : the one associated with the current density perturbation $\mathbf{J}_1^\star$, and the one associated to the resonant particles $\mathbf{J}_1^\dagger$ (since the plasma will respond to the perturbation).

The shape of the distribution function in a Harris layer is given by the Eq. (1.50). It is still valid for the case of tearing mode because the canonical momentum P_z is always a Hamiltonian invariant. It is then necessary to take into account the perturbed part of the vector potential. This one being small, one can make a Taylor expansion at first order of the distribution given by Eq. (1.50) to get the distribution function of the specie s at first order $f_{1s}^\star$

$$f_{1s}^\star = \frac{q_s}{k_B T_s}\mathbf{V}_s.\,\mathbf{A}_1(x, y, t) f_{0s}(y, \mathbf{v}) \tag{1.90}$$

Exercize 7. *Using the form of $A_0(y)$ given by Eq. (1.60), show that the sum on the species s of the moments of order 1 of $f_{1s}^\star$ gives*

$$\mathbf{J}_1^\star = \frac{2}{\mu_0 L^2 \cosh^2(y/L)} A_1 \widehat{\mathbf{z}} \tag{1.91}$$

To get $\mathbf{J}_1^\dagger$ associated with the Čerenkov effect, you have to solve the Vlasov equation to get $f_{1s}^\dagger$. This calculation can only be done for the species s in the region $|y| < l_s$: the magnetic field of order 0 is very small (the particles are demagnetized). The Vlasov equation of order 1 can be solved with the method of the characteristics ; it is written [2]

$$\frac{\partial f_{1s}}{\partial t} + \mathbf{v}.\frac{\partial f_{1s}}{\partial \mathbf{r}} = -\frac{q_s}{m_s}\left[-\frac{\partial \mathbf{A}_1}{\partial t} + \mathbf{v} \times (\boldsymbol{\nabla} \times \mathbf{A}_1)\right].\frac{\partial f_{0s}}{\partial \mathbf{v}} \tag{1.92}$$

The last term of the right-hand side is associated with the evolution of $f_{1s}^\star$ (the magnetic force does not work). The first is therefore associated with the electric force, and thus with the evolution of $f_{1s}^\dagger$. This equation is therefore written

$$\frac{\partial f_{1s}^\dagger}{\partial t} + \mathbf{v}.\frac{\partial f_{1s}^\dagger}{\partial \mathbf{r}} = \frac{q_s}{m_s}\frac{\partial \mathbf{A}_1}{\partial t}.\frac{\partial f_{0s}}{\partial \mathbf{v}} \tag{1.93}$$

The right-hand side is integrated using the characteristics method along an undisturbed orbit :

$$f_{1s}^\dagger = \int_{-\infty}^{t} \frac{\imath\omega q_s}{k_B T_s} A_1(y) v_z f_{0s}(y, \mathbf{v}) e^{-\imath[\omega\tau - kx(\tau)]} d\tau \tag{1.94}$$

[2] As for the Harris sheet, an electrostatic potential that is identically zero in the whole domain is a solution ... and this is the one that we choose therefore

The orbit $x(\tau)$ of a particle in the undisturbed field is simple : being demagnetized, the equation of its motion is $x(\tau) = v_x\tau$. It is further assumed that for each specie s, the resonant particles are in the $|y| < l_s$ layer, which implies that $A_1(y)$ can be considered as constant. We can therefore take this term out of the integral, as well as the order 0 of the distribution function (for the same reason). The integral therefore relates only to the exponential term,

$$f_{1s}^{\dagger} = \frac{-\omega q_s}{k_B T_s} A_1(y) v_z f_{0s}(y, \mathbf{v}) \frac{1}{\omega - k v_x} e^{-\imath(\omega - k v_x)t} \tag{1.95}$$

The function $f_{1s}^{\dagger}$ has a single pole at the Čerenkov resonnance ($v_x = \omega/k$). To calculate its first order moment, one has to define this function on all $\mathbb{C}$ by analytic continuation, and use the residue theorem to calculate the integral of $f_{1s}^{\dagger}$ to get the current. By summing on the species s and using Plemelj's formula,

$$J_{1z}^{\dagger} = \sum_s \frac{\omega q_s^2}{k_B T_s} A_1(y) \iiint_{\mathbb{R}^3} v_z^2 f_{0s}(y, \mathbf{v}) \imath\pi\delta(\omega - k v_x) d\mathbf{v} \tag{1.96}$$

Exercize 8. *Show that this integral can be written*

$$\mathbf{J}_1^{\dagger} = \sum_s -\imath\pi^{1/2} \frac{\omega_{Ps}^2}{\mu_0 c^2} \frac{\omega}{|k| v_{Ts}} A_1(y) \widehat{\mathbf{z}} \tag{1.97}$$

The form of $J_{1z}^{\dagger}$ is only valid for $|y| < l_s$. Outside this layer, the particles are magnetized and can not satisfy the Čerenkov effect, ie $\mathbf{J}_{1s}^{\dagger} = 0$. Returning to the Maxwell-Faraday equation,

$$\frac{d^2 A_1(y)}{dy^2} - \left[k^2 + \Psi_0(y) + \sum_s \Psi_s(y, \mathbf{k}, \omega)\right] A_1(y) = 0 \tag{1.98}$$

with

$$\Psi_0 = -\frac{2}{L^2 \cosh^2(y/L)} \ , \ \Psi_s = \begin{cases} -\imath\pi^{1/2} \dfrac{\omega}{|k| v_{Ts}} \dfrac{\omega_{Ps}^2}{c^2} & |y| < l_s \\ 0 & |y| > l_s \end{cases} \tag{1.99}$$

In Eq. (1.98), the first term in the brackets is the Laplacian in the x direction, the second one is equal to $\mu_0 \mathbf{J}_1^{\star}$ and the third one is equal to $\mu_0 \mathbf{J}_1^{\dagger}$. The problem is thus to solve a Schrödinger equation in a potential Ψ_0 supperposed to a thin potential well $\sum_s \Psi_s$ in its center. We then have to find the form of $A_1(y)$ in and out of Ψ_s, and then connect these 2 solutions. In the region where Ψ_s is null (out of the current layer), the solution must satisfy $A_1(y) \to 0$ for $y \to \pm\infty$, and is (see [White et al., 1977])

$$A_1(y) = A_1(0) \left[1 + \frac{\tanh(|y|/L)}{kL}\right] e^{-k|y|} \tag{1.100}$$

The solution of $A_1(y)$ in the region where at least one of the Ψ_s is not negligible is more hard, and can only be done in simple cases. Considering that the potential Ψ_e is constant in $|y| < l_e$, the solution of the Maxwell-Faraday equation is (by obviously omitting adiabatic contributions Ψ_0 as well as those of protons Ψ_p, which is justified if Ψ_e is large enough)

$$A_1(y) = A_1(0)\cosh(\Psi_e^{1/2} y) \tag{1.101}$$

which is a solution of $d^2_{y^2} A_1 - \Psi_e A_1 = 0$.

It remains to ensure the continuity of the two solutions (1.100) and (1.101) at the border $y = \pm l_e$, which can be done by equalizing the logarithmic derivatives

$$\frac{1 - k^2 L^2}{kL^2 + l_e} = \Psi_e^{1/2} \tanh(\Psi_e^{1/2} l_e) \tag{1.102}$$

We can do a Taylor's expansion, l_e being small, to get the value of Ψ_e

$$\Psi_e = \frac{1 - k^2 L^2}{kL^2} \frac{1}{l_e} \tag{1.103}$$

By matching this expression to that obtained in the Eq. (1.99) for $\Psi_s (s = e)$

$$\Psi_e = -\imath \pi^{1/2} \frac{\omega}{|k| v_{Te}} \frac{\omega_{Pe}^2}{c^2} \tag{1.104}$$

This expression is real only if $\omega = \imath\gamma$ is purely imaginary. The growth rate γ of the tearing mode is thus given by

$$\pi^{1/2} \frac{\gamma}{v_{Te}} \frac{\omega_{Pe}^2}{c^2} = \frac{1 - k^2 L^2}{L^2} \frac{1}{l_e} \tag{1.105}$$

Exercize 9. *Show that the pressure balance across the layer can be rewritten as a function of c/ω_{Pe} (the electron inertial length)*

$$\left[\frac{c}{\omega_{Pe}}\right]^2 = 2\left[1 + \frac{T_p}{T_e}\right] \rho_e^2 \tag{1.106}$$

In developing, we obtain the expression of the growth rate given by [Coppi et al., 1966]

$$\gamma = \left[1 + \frac{T_p}{T_e}\right]^2 \left[\frac{c}{\omega_{Pe}}\right]^{5/2} \frac{\Omega_e}{\pi^{1/2}} (1 - k^2 L^2) \tag{1.107}$$

Many scientific communities paid attention to this result. In particular, it was a scenario to explain the triggering of the magnetospheric substorms associated with the injection of particles in auroral zones responsible for the northern lights. But this enthusiasm has been restrained.

The growth rate of the tearing mode is large at small k, but decreases to saturate at $kL = 1$. During the growth of this mode, the magnetic islands of Fig. 1.5 will therefore reach a quasi-circular form. The current layer being thin, this mode will saturate very quickly, not allowing to reconnect a lot of magnetic flux. Moreover, [Lembege and Pellat, 1982] have shown that a normal component of the magnetic field (in the Y direction), even weak, allows to magnetize the electrons and to thus stabilize the configuration.

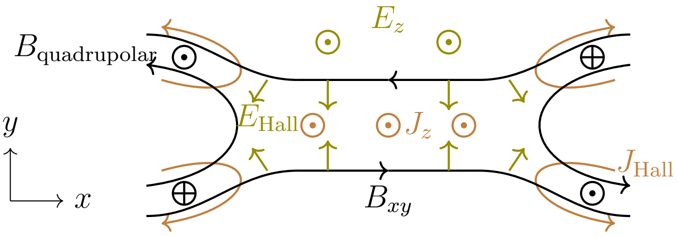

Figure 1.8: Structure of the magnetic field, electric field and current during fast reconnection.

The limit between collisional and collisionless tearing (also called two-fluid transition criteria, see *e.g.* [Cassak et al., 2005]) is $\delta \lesssim d_i$ for a weak guide-field or $\delta \lesssim \rho_s$ for a strong guide-field. This limit has also been predicted numerically by [Simakov and Chacón, 2008].

As a consequence, the thining of the CS can mean that reconnection will fall in the kinetic regime.

The Hall term in the Ohm's law is then fundamental in controlling the (fast) reconnection rate (BIRN2001). For $\delta \lesssim d_i$, Hall term will lead, so the reconnection will be whistler mediated.

Inside the CS, E field is mainly associated to the field reversal, ie $E_y = J_0 B_0$ (directed toward the mid-plane). At the tips of the separatrices (outer from the CS), this E-field is no more curl-free. In polar coordinates, $\partial_t B_z = +\partial_\theta E_r (\equiv E_y)$ so a quadrupolar B_z pattern develops. There is an in-plane current J_{xy} associated to the Hall quadrupolar B-field, carried by the e^- along the separatrices. Then e^- are flowing toward the X-point along the upstream side of the separatrices. They then get out from the X-point flowing along the downstream side of the separatrices. Close enough to the mid-plane, U vanishes so E_z is mainly resulting from the Hall $J_{xy} \times B_{xy}$ term.

Large-scale full-PIC simulations ([Shay et al., 2007]) showed that the asymptotic reconnection rate is independent of m_e and of the system size. Such Hall reconnection observed both in-situ ([Nagai et al., 2001]) and in laboratory ([Yamada et al., 2006]).

Fast reconnection is also at play in electron-positron plasma where Hall effect is not operative ([Bessho and Bhattacharjee, 2005]), which keeps open the question of the importance of the Hall effect in fast reconnection.

Aside from the Hall quadrupolar magnetic field, there is an other important observational feature associated to fast reconnection : an "electron depletion layer" develops along the separatrices where the e^- and p^+ density strongly decrease ([Shay, 1998]).

Bibliography

[Bessho and Bhattacharjee, 2005] Bessho, N. and Bhattacharjee, A. (2005). Collisionless reconnection in an electron-positron plasma. *Phys. Rev. Lett.*, 95(24):245001.

[Cassak et al., 2005] Cassak, P. A., Shay, M. A., and Drake, J. F. (2005). Catastrophe model for fast magnetic reconnection onset. *Phys. Rev. Lett.*, 95(23):235002–+.

[Coppi et al., 1966] Coppi, B., Laval, G., and Pellat, R. (1966). Dynamics of the geomagnetic tail. *Phys. Rev. Lett.*, 16:1207–1210.

[Daughton et al., 2009] Daughton, W., Roytershteyn, V., Albright, B. J., Karimabadi, H., Yin, L., and Bowers, K. J. (2009). Influence of coulomb collisions on the structure of reconnection layers. *Phys. Plasmas*, 16(7):072117–+.

[Dungey, 1961] Dungey, J. W. (1961). Interplanetary magnetic field and the auroral zones. *Phys. Rev. Lett.*, 6:47–48.

[Furth et al., 1963] Furth, H. P., Killeen, J., and Rosenbluth, M. N. (1963). Finite-Resistivity Instabilities of a Sheet Pinch. *Physics of Fluids*, 6:459–484.

[Giovanelli, 1947] Giovanelli, R. G. (1947). Magnetic and electric phenomena in the sun's atmosphere associated with sunspots. *Monthly Notices of the Royal Astronomical Society*, 107(4):338–355.

[Harris, 1962] Harris, E. (1962). On a plasma sheath separating regions of oppositely directed magnetic field. *Il Nuovo Cimento (1955-1965)*, 23:115–121.

[Krauss-Varban and Omidi, 1995] Krauss-Varban, D. and Omidi, N. (1995). Large-scale hybrid simulations of the magnetotail during reconnection. *Geophys. Res. Lett.*, 22:3271–3274.

[Lazarian and Vishniac, 1999] Lazarian, A. and Vishniac, E. T. (1999). Reconnection in a weakly stochastic field. *The Astrophysical Journal*, 517(2):700–718.

[Lembege and Pellat, 1982] Lembege, B. and Pellat, R. (1982). Stability of a thick two-dimensional quasineutral sheet. *Phys. Fluids*, 25:1995–2004.

[Loureiro et al., 2005] Loureiro, N. F., Cowley, S. C., Dorland, W. D., Haines, M. G., and Schekochihin, A. A. (2005). X-point collapse and saturation in the nonlinear tearing mode reconnection. *Phys. Rev. Lett.*, 95(23):235003.

[Loureiro et al., 2012] Loureiro, N. F., Samtaney, R., Schekochihin, A. A., and Uzdensky, D. A. (2012). Magnetic reconnection and stochastic plasmoid chains in high-lundquist-number plasmas. *Phys. Plasmas*, 19(4):042303.

[Machida et al., 1994] Machida, S., Mukai, T., Saito, Y., Hirahara, M., Obara, T., Nishida, A., Terasawa, T., and Maezawa, K. (1994). Plasma distribution functions in the Earth's magnetotail ($X_{GSM} \sim$ -42R_E) at the time of a magnetospheric substorm: GEOTAIL/LEP observation. *Geophys. Res. Lett.*, 21(11):1027–1030.

[Nagai et al., 2001] Nagai, T., Shinohara, I., Fujimoto, M., Hoshino, M., Saito, Y., Machida, S., and Mukai, T. (2001). Geotail observations of the Hall current system: Evidence of magnetic reconnection in the magnetotail. *J. Geophys. Res.*, 106(A11):25929–25950.

[Parker, 1957] Parker, E. N. (1957). Sweet's mechanism for merging magnetic fields in conducting fluids. *J. Geophys. Res.*, 62:509–520.

[Petschek, 1964] Petschek, H. E. (1964). *Magnetic Field Annihilation*, volume 50, page 425.

[Rutherford, 1973] Rutherford, P. H. (1973). Nonlinear growth of the tearing mode. *Physics of Fluids*, 16:1903–1908.

[Shay, 1998] Shay, M. A. (1998). *The dynamics of collisionless magnetic reconnection*. PhD thesis, UNIVERSITY OF MARYLAND COLLEGE PARK.

[Shay et al., 2007] Shay, M. A., Drake, J. F., and Swisdak, M. (2007). Two-scale structure of the electron dissipation region during collisionless magnetic reconnection. *Phys. Rev. Lett.*, 99(15):155002–+.

[Simakov and Chacón, 2008] Simakov, A. N. and Chacón, L. (2008). Quantitative, comprehensive, analytical model for magnetic reconnection in hall magnetohydrodynamics. *Phys. Rev. Lett.*, 101:105003.

[Sweet, 1958] Sweet, P. A. (1958). The Neutral Point Theory of Solar Flares. In Lehnert, B., editor, *Electromagnetic Phenomena in Cosmical Physics*, volume 6 of *IAU Symposium*, page 123.

[Ugai, 1999] Ugai, M. (1999). Computer studies on the spontaneous fast reconnection model as a nonlinear instability. *Physics of Plasmas*, 6(5):1522–1531.

[White et al., 1977] White, R. B., Monticello, D. A., Rosenbluth, M. N., and Waddell, B. V. (1977). Saturation of the tearing mode. *Physics of Fluids*, 20:800–805.

[Yamada et al., 2006] Yamada, M., Ren, Y., Ji, H., Breslau, J., Gerhardt, S., Kulsrud, R., and Kuritsyn, A. (2006). Experimental study of two-fluid effects on magnetic reconnection in a laboratory plasma with variable collisionality. *Physics of Plasmas*, 13(5):052119.